

EFFECTS OF RADIATION ENVIRONMENT ON REUSABLE NUCLEAR SHUTTLE SYSTEM

A. G. Lane

Space Division, North American Rockwell

Since radiation protection for a manned nuclear rocket represents the most significant design constraint, major emphasis has been placed upon parametric tradeoff analyses of a wide spectrum of alternate tank configurations to minimize both primary and secondary, direct and scattered radiation sources emanating from the NERVA (nuclear engine for rocket vehicle application). The analytical approach utilizing point kernel techniques is described and detailed data are presented on the magnitude of neutron/gamma doses for different locations. Dose rates are presented for both engine firing and post-shutdown periods. Conical aft bulkhead geometries employing a range of included half cone-angles from 5-15 degrees and end cap radii from 25 to 125 inches were evaluated. Single-tank configurations utilizing smaller cone angles and end cap radii were found to minimize integral radiation levels, hence, stage shielding-weight penalties for shuttle missions. This is due to the greater payload separation distance, reduction of the effective energy disposition and scattering centers in the aft end of the tank, and greater depth of the liquid hydrogen propellant for radiation attenuation at any given time during the draining cycle for a fixed tank propellant capacity. Hybrid configurations employing an upper tank with a reduced cone angle and end cap radius results in low integral payload doses primarily due to the increased separation distance caused by the elongation of the larger capacity upper tank. A preliminary radiation damage assessment is discussed of possible reusable nuclear shuttle (RNS) materials, components, and subsystems, and the possible effects of the radiation environment on various phases of RNS mission operations, i.e., maintenance, rendezvous, docking, and engine disposal.

One of the major problems in designing nuclear propulsion vehicles is providing adequate shielding from the system's radiation environment. The prime mover behind the design definition of the reusable nuclear shuttle (RNS) has been the design of configurations that minimize neutron and gamma radiation levels to the man-rated payloads and radiation sensitive components and subsystems.

Since radiation protection for a manned payload represents the most serious design constraint, a major emphasis has been placed upon a parametric tradeoff analyses of a wide spectrum of alternate tank configurations to minimize primary and secondary, direct and scattered radiation sources emanating from the NERVA engine.

The discussion of tank configurations presented in this paper is primarily concerned with two promising classes of RNS configurations recently evaluated; (1) a single conical tank configuration employing aft bulkhead geometries with included half cone-angles less than 15 degrees and closing end-cap radii from 25 to 125 inches, and (2) hybrid configurations employing a separate large-capacity propellant module which includes a smaller capacity, small diameter propellant tank adjacent to the NERVA engine.

Also discussed are the possible effects of the radiation environment for a selected RNS vehicle configuration on various mission operations for a reference lunar shuttle mission.

Finally, a preliminary radiation damage assessment of candidate RNS materials, components, and subsystems for a selected candidate vehicle configuration is briefly reviewed. The damage assessment is based upon requirements for a maximum 10-hour NERVA engine operation imposed by engine design requirements.

ANALYSIS APPROACH TO TANK CONFIGURATIONS

The majority of the radiation calculations for this study were performed utilizing point kernel techniques on the IBM 360, model 65 computer system at North American Rockwell's Space Division. The point kernel techniques represent the most efficient and least costly method of preliminary analysis of the radiation environment of a wide variety of nuclear stage configurations and tank geometries. A flow chart summary of the computational methods employed in this study is shown in Figure 1.

The QAD-B and GR-34 point kernel programs, originally developed by LASL (Reference 1), were the basic tools employed in the analysis. The Space Division version of the QAD-B program is designed to calculate neutron or gamma radiation levels at detector points located within or outside a complex radiation source geometry which can be described by a combination of quadratic surfaces. The program evaluates the material thicknesses intercepted along the line-of-sight from the source point to the detector point. These material thicknesses or path lengths then are

employed in attenuation functions to calculate the multigroup flux levels, dose rates, or heating rates at the detector. The attenuation function for gamma rays employs exponential attenuation with an infinite medium buildup factor. Two neutron attenuation functions are included: (1) a modified Albert-Welton function for calculating fast neutron dose rates using removal cross-sections and (2) a monovariant polynomial expression for computing neutron spectra and dose rates using infinite media moments data.

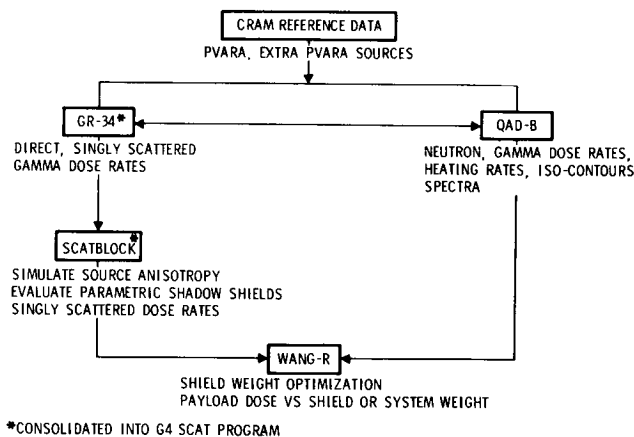


Figure 1. Computational Methodology

The Space Division version of the GR-34 program calculates the direct gamma radiation levels from a point source to a point detector as in QAD. Similarly, the attenuation function for gamma rays also employs exponential attenuation with infinite medium buildup factors. Hence, the difference between the direct radiation levels with buildup and without buildup, can be taken (in most instances) to be a somewhat conservative estimate of the scattered radiation level. However, the GR-34 program allows a calculation of the first photon or gamma ray scattering event analytically. The scattering medium for the first photon collision is described by a series of spatial points representing volume elements. Gamma scattering prediction is based on multigroup Klein-Nishina differential angular cross-sections. The source energy groups are degraded according to the Compton relationship of energy ratio versus scattering angle. A scattering event contribution is calculated for each volume element and the gamma levels at the detector point are generated by summing contributions from the first scattering event. The radiation levels may be calculated for cases either with or without the application of an infinite medium buildup factor along the scattered leg. Thus, the GR-34 is analogous to the Monte Carlo method for treating line sources until the occurrence of the first collision event.

The SCATBLOCK program, originally developed by Aerojet Nuclear Systems Company (Reference 2), has been modified by Space Division and is included as an optional subroutine within the GR-34 program. The resulting program which requires no tapes is called G4 SCAT. SCATBLOCK uses an array of scattered gamma dose rates calculated by the main program and calculates gamma kerma rates when disk shields of arbitrary location and radius are placed between the source and scatter points. This allows the calculations necessary for the design of a scatter gamma shield to be carried out parametrically for each shield configuration without the complicated problem setups and longer computer run times of the more general G4 SCAT or QAD-B programs.

The WANG-R is a Space Division modification of a program originally developed by Aerojet Nuclear Systems Company (Ref. 2) which is used to generate values of integral radiation doses as a function of shield and/or system weight. The principal input parameters are doses from individual PVARA (pressure vessel and reactor assembly) and from sources external to PVARA, tables of shield weight as a function of size, and matrices of transmission factors for each source as a function of shield size. Since these inputs are easily varied, parametric shield studies may be accomplished rapidly and inexpensively.

Mathematical models for the various tank propellant configurations were sized for an initial LH₂ propellant capacity of 300,000 pounds with an LH₂ residual capacity of 5000 pounds after engine shutdown for post-shutdown cooling requirements. Tank propellant drainage curves were developed on the basis of a nominal LH₂ flow rate of 91.4 pound-second⁻¹. A 3300-pound internal engine shield was assumed for all calculations. The G4 SCAT point kernel program was utilized in the determination of tank-top gamma kerma rates from both PVARA and external sources.

An extrapolation of the multiregion PVARA volume source to a single point source at the core midplane, as well as the utilization of anisotropy factors for the PVARA point source extrapolations, was the general technique employed in the current analysis for PVARA source contributions to tank top integral dose. A more detailed discussion of technique may be found in Reference 3. Identical photon thirteen-group energy structures, energy spectrums, and source strengths were utilized in all calculations.

Multigroup source data for the external sources analyzed, i.e., the PDL (pump discharge line) and TCA (thrust chamber assembly) were developed from the CRAM data (Reference 4).

The multipoint source distributions in this reference were collapsed into three effective PDL sources and four effective TCA sources, respectively. Similarly, the LH₂ capture gamma sources were derived for four effective point sources.

The integral-tank top gamma doses represent the summation of each effective source contribution for the three aforementioned external sources.

The general geometry model for the various tank configurations is shown in Figure 2. The on-axis separation distance from the PVARA midplane to the tank bottom was 200 inches for all tank configurations evaluated.

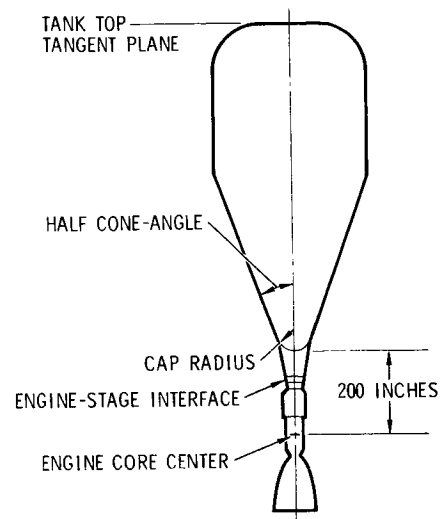


Figure 2. Tank Configurations Geometry Model

SINGLE CONICAL TANK CONFIGURATIONS

Early RNS parametric design analyses as discussed in Reference 5 led to the preliminary conclusion that the optimum single tank configuration for manned applications was one employing an aft bulkhead geometry with an eight-degree half cone-angle and an end cap radius of 25 inches.

The shield weight data utilized in the parametric tradeoff analyses was derived from this preliminary screening which considered tank top dose contributions from the PVARA source. Conical aft bulkhead configurations were evaluated that employed varying half cone-angles of 5 to 15 degrees and end cap radii of 25, 50, 75, and 100 inches.

However, a more detailed analysis of selected single-tank conical configurations was undertaken to substantiate the results of the preliminary screening analysis. The computations were performed with the G4 SCAT point kernel program for tank configurations with an initial LH₂ capacity of 300,000 pounds. More detailed drainage curves were developed based on the evaluation of tank-top gamma kerma rates at five representative propellant levels during the course of the tank drain.

Comparisons of the more detailed calculations for PVARA tank top dose with similar results obtained during the preliminary screening analysis confirmed the effectiveness of the earlier approach (Table 1).

The more detailed G4 SCAT point kernel calculations for both PVARA and external source contributions are shown in Table 2 for single tank conical configurations with aft bulkhead geometries employing half cone-angles of 8, 10, 12, and 15 degrees and end cap radii of 25, 50, 75, and 100 inches. The on-axis tank-top integral gamma dose values in Table 2 represent the summation of the PVARA and external source contributions. The aforementioned dose values are all based on the common assumptions of an initial LH₂ tank capacity of 300,000 pounds, a terminating LH₂ residual of 5,000 pounds at engine shutdown, and a 3300-pound internal NERVA shield. Similarly, the relative gamma kerma levels are displayed in Figure 3 as a function of varying half cone-angles from 8 to 15 degrees and end cap radii extending from 25 to 100 inches. Both Figure 3 and Table 2 further substantiate the results of the earlier preliminary screening analysis which indicated three reasons that single tank conical configurations with aft bulkhead geometries employing both reduced half cone-angles and end cap radii minimize integral tank top dose for a fixed propellant capacity: (1) greater source-to-tank top detector separation distance, (2) reduced effective energy deposition and scattering centers in the aft end of the propellant tank, and (3) greater depths of the LH₂ propellant column for radiation attenuation at any specified time during the tank draining cycle. For example, the single tank configuration employing an eight-degree half cone-angle and 25-inch end cap radius exhibits a source-to-detector separation distance of 561 inches greater than a configuration employing a

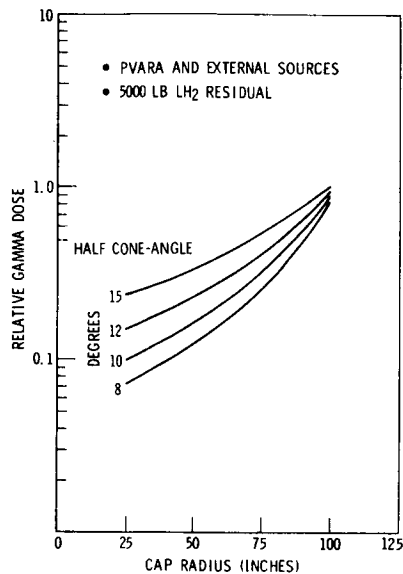


Figure 3. Relative Dose Variation with Conical Tank Geometries

15-degree, 100-inch cap radius for a fixed LH₂ tank capacity of 300,000 pounds. Additionally, the depth of the LH₂ column at the end of the engine burn (5000-pound LH₂ residual) is 198 inches greater for an eight-degree half cone-angle, 25-inch end cap radius aft bulkhead geometry than a conical configuration employing a 15-degree half cone-angle, 100-inch end cap radius. This increased column depth represents approximately two photon relaxation lengths in LH₂.

Additionally, an extension of the analysis to a cap radius of 125 inches would demonstrate that the tank-top integral dose values tend to converge at this radius regardless of the half cone-angle since the three principal factors described become nearly equivalent in a practical sense. This premise is evidenced in Table 2 which shows a variation in tank length of only 85 inches (1,297 inches to 1,212 inches) at a cap radius of 125 inches over the range of half cone-angles from 8 to 15 degrees. Similarly, the depth of the LH₂ column near the termination of the tank drain tends to converge near a cap radius of 125 inches (Figure 4) for a propellant level of 7500 pounds near the end of the engine firing. Hence, the drainage rate histories are nearly equal during the time interval where the most significant portion of the total tank top integral dose is accumulated. Additionally, the geometric surface area and, consequently, the energy deposition near the tank bottom is controlled principally by the magnitude of the end cap radius for large values of cap radii, within the range of the evaluated half cone-angles.

The parametric data also illustrates the dominating influence of reduction in cap radius on minimizing the tank top integral dose. For example, it is shown in Figure 3 that the aft bulkhead geometry employing an 8-degree half cone-angle and a 25-inch end cap radius lowers the tank top integral dose. However, the aft bulkhead geometry employing a 10-degree half cone-angle and 25-inch end cap radius has about a 20-percent lower relative tank top integral dose than an aft bulkhead geometry employing an 8-degree half cone-angle and a 50-inch end cap radius although the tank lengths are approximately equal for the two configurations as shown in Table 2. This effect is principally due to the longer LH₂ column and, hence, great shielding effectiveness afforded by the smaller 25-inch cap radius during the latter stages of the tank drain cycle.

In order to determine whether an appreciable "viewing" effect around the shadow of the LH₂ column occurs in the 8-degree half cone-angle geometry employing the 25-inch end cap radius, PVARA and PDL tank top integral doses were evaluated at radial detector locations of 132.5 and 196.85 inches, respectively. Comparisons with on-axis tank integral doses are shown in Table 3 for an axial detector location 2067 inches above the core's midplane and LH₂ residual of 5000 pounds. The PVARA tank top integral doses are shown to increase from 22.6 rem on axis to 26.5 rem near the outer radius of the tank, a factor of about 1.16. Similarly, the PDL tank top integral dose varies from 6.58 rem on axis to 8.41 rem near the outer radius of the tank, a factor of about 1.28.

Table 1. PVARA On-Axis Tank Top Integral Dose Comparisons

Aft Bulkhead Geometry		LH ₂ Residual (lbs)	G4 SCAI Analysis (rem/11)	Preliminary Screening Analysis (rem/11)	Ratio (2/11)
Cone Half-Angle (degrees)	Cap Radius (inches)				
8	50	7500	42.3	38.4	0.908
		5000	50.8		
8	25	7500	16.9	12.3	0.728
		5000	22.6		
5	50	7500	28.3	27.1	0.958
		5000	45.4		
15	100	7500	469.4	561.0	1.191
		5000	534.1		
		0	714.6		

Table 2. Tank Top Dose Comparison for Conical Geometries

Cap Radius (in.)	Cone Half-Angle (degrees)																	
	15				12				10				8					
	125	100	75	50	100	75	50	25	125	100	75	50	25	125	100	75	50	25
Tank Length (in.)	1212	1266	1327	1394	1464	1536	1608	1688	1775	1868	1967	2072	2182	2297	2427	2572	2732	2907
Gamma Dose (rem)	520	275	172	125	473	208	120	78	442	177	86	52	432	130	65	38	28	18

Table 3. Tank Top Radiation Dose Variation

Radiation Source	Integral Tank Top Dose (rem)		
	Radial Detector Location (inches)		
PVARA	0	132.5	196.85
	22.6	24.7	26.5
PDL	6.58	7.14	8.41

External disk-shield weight variations with end cap radius and half cone-angle for the single tank conical configurations are shown in Figure 5 for a tank-top integral dose criterion of 10 rem. Aft bulkhead geometries employing half cone-angles from 8 to 15 degrees and end cap radii from 25 to 100 inches were evaluated.

The external shield weights were derived from the data for the on-axis integral dose (both PVARA and external sources) shown in Table 2. The external disk shield weights are shown to vary from about 4,000 pounds for the 8-degree half cone-angle and 25-inch end cap radius aft bulkhead geometry, to about 13,000 pounds for a 15-degree half cone-angle, 100-inch end cap radius aft bulkhead geometry using a 10-rem tank top dose criterion. As expected, the external shield weight curves shown in Figure 5 have similar characteristics to their counterpart, the relative tank-top dose plots shown in Figure 3 as a function of half cone-angle and end cap radius.

COMPARISON OF RNS CONFIGURATION CLASSES

The previously discussed parametric analysis of single conical tank configurations established the basis for comparison of three classes of candidate RNS tank configurations: single tank conical, modified dual cell, and hybrid (shown in Figure 6). It has been established that the aft bulkhead geometry is the dominant factor in reduction of the tank top dose for a fixed LH₂ tank capacity, internal engine shield, and separation distance between the engine (reactor core) midplane and tank bottom.

Three tentative baseline configurations representing the three comparison classes are:

1. Single-tank conical configuration, employing an 8-degree half cone-angle and a 25-inch end cap radius
2. Modified dual-cell configuration, employing the single-tank aft bulkhead geometry of (1) with a "shortened" 50-inch radius inner cell
3. Hybrid dual-tank configuration, employing a small tank (9300 pound LH₂ capacity) that interfaces with the NERVA engine and a larger tank (290,000 pound LH₂ capacity) utilizing an aft bulkhead geometry with an 8-degree half cone-angle with a 40-inch end cap radius.

The evaluation of the tank-top integral direct and scattered gamma dose contributions from both the PVARA and external sources for the three configurations is summarized in Table 4.

Table 4. On-Axis Tank Top Radiation Dose Summary

Tank Design	8 Degree, 25-Inch R Cap, Single Tank	8 Degree, 25-Inch R Cap, Modified Dual Cell	8 Degree, 40-Inch R Cap Hybrid
PVARA direct	10.1	8.7	27.1
PVARA scattered	12.5	13.1	45.3
PVARA total	22.6	21.8	72.4
LH ₂ capture	7.2	7.2	7.0
TCA direct	0.62	0.71	1.03
TCA scattered	1.03	1.13	1.54
PDL direct	3.14	2.98	3.12
PDL scattered	3.44	3.51	2.58
TPA total	(8.77)*		
	38.03 (46.80)	37.33	87.67

*Off-axis radial detector location at 132.5

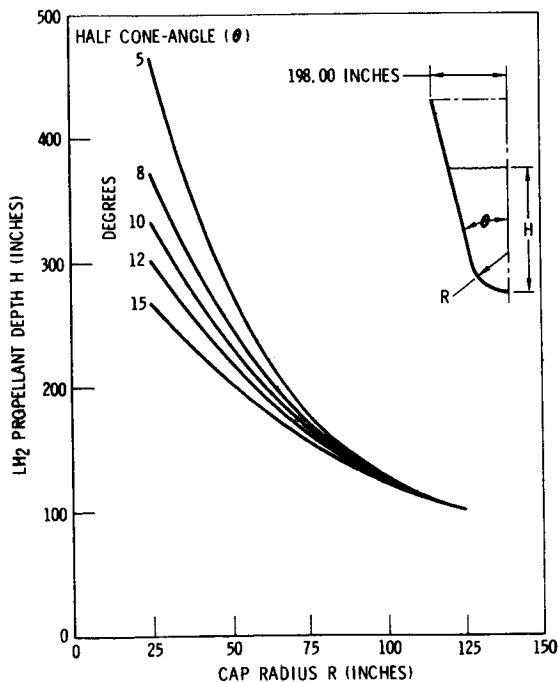


Figure 4. Residual Propellant Level for 7500-Pound Residual LH₂

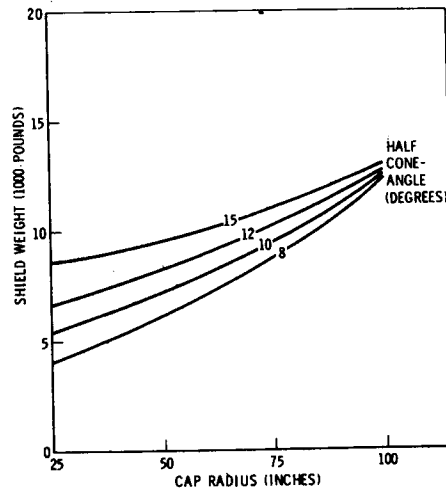


Figure 5. Shield Weight Variation for Single Tank Conical Configuration

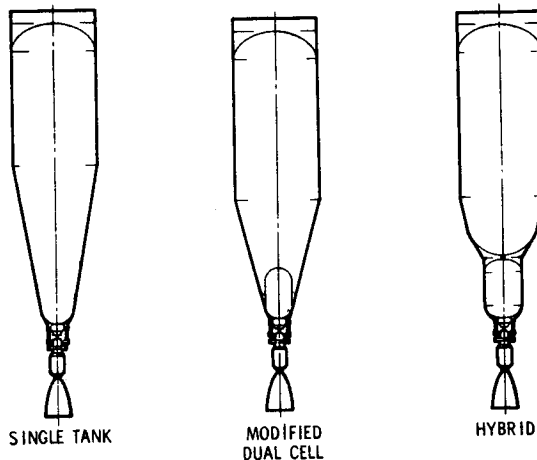


Figure 6. RNS Tank Configuration Classes

SINGLE-TANK CONICAL CONFIGURATION

The table shows the increased relative importance of the external source contributions to the total dose for the single conical tank configuration. The external source contributions represent about 43 percent of the total on-axis tank top integral dose of 38 rem. This point is illustrated in Figures 7 and 8, which depict on-axis tank-top gamma kerma rates and integral gamma doses, respectively, as a function of time prior to completion of the tank drain for the 8-degree, 25-inch conical tank geometry.

A Monte Carlo analysis of this tank configuration (Reference 6) generally confirms Space Division's assessment of the influence of half cone-angle and end cap radius on tank top radiation levels.

MODIFIED DUAL-CELL CONFIGURATION

The modified dual-cell configuration employs the 8-degree half cone-angle, 25-inch end cap radius, aft bulkhead geometry with a shortened inner cell of 50-inch radius and an "effective" column length of 427 inches from the tank bottom at the vertical midplane. The inner cell can contain 5950 pounds of LH₂. This particular dual cell design precludes any neutron dose contributions at tank top since the aft bulkhead is completely immersed in LH₂ during the engine burn to an LH₂ residual of 5000 pounds. The on-axis integral tank top doses are comparable to those obtained for the single-tank conical configuration (Table 4). Slight differences were obtained in PVARA direct and PVARA scattered contributions. The PVARA direct gamma dose is about 13 percent lower for the dual cell due to a small increase in the depth of the LH₂ column near the end of the tank drain cycle. The increase in depth at the 5000-pound LH₂ residual level is about 34 inches, or less than one-third of a photon relaxation length in LH₂. Little difference was noted in the PVARA gamma scattered dose.

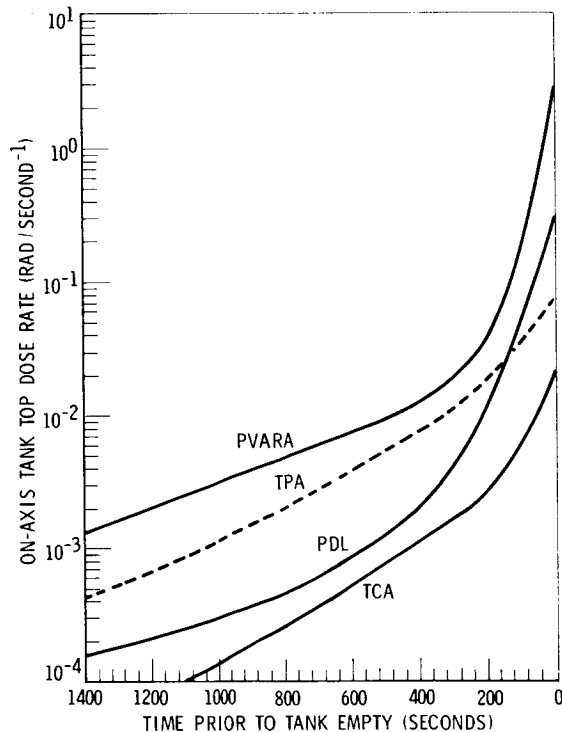


Figure 7. Conical-Tank Radiation Dose Rate Variations

Since the tank drain history for the modified dual-cell configuration parallels that of the single-tank conical configuration to the 5950-pound LH₂ level, only about 10 seconds is available for secondary gamma scattering effects in the GH₂ in the region between the outer boundary of the inner cell and the inner boundary of the outer tank wall prior to engine shutdown with an LH₂ residual of 5000 pounds. Additionally, there are fewer scattering centers available due to the drastically reduced volume of the region between the inner cell and outer tank (small cone angle and small, cap radius aft-bulkhead geometry). However, the modified dual-cell configuration has additional structural weight penalties of 1275 pounds (added complexity of the inner cell design as indicated in Reference 7). Thus, the modified dual-cell configuration offers no particular advantages in radiation shielding for RNS applications when compared to its single tank counterpart.

HYBRID DUAL-TANK CONFIGURATION

In the hybrid configuration, the on-axis tank-top PVARA integral gamma dose of about 72 rem represents about 82 percent of the total integral tank-top dose of about 88 rem (Table 4 and Figures 9 and 10).

The hybrid configuration exhibits appreciably higher PVARA direct and scattered integral gamma-dose levels than either the single-tank or modified dual-cell configurations irrespective of an increased source-to-detector separation distance of about 209 inches. However, the energy deposition and available scattering centers are greater in the aft tank for the hybrid configuration primarily due to its 77-inch end cap radius. Concomitantly, the LH₂ level in the tank is less at any given time during the engine burn and tank drain. For example, the 5000 pound LH₂ residual level is about 176 inches less in the hybrid tank than it is for the baseline single-tank conical configuration. This residual level is only about three inches greater than a single tank configuration employing the 8-degree, 75-inch end cap radius, aft bulkhead geometry. The shielding effectiveness

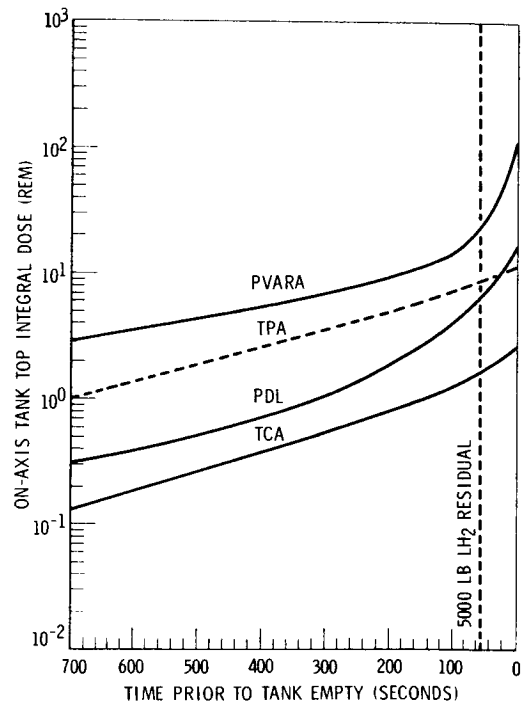


Figure 8. Conical-Tank Integral Radiation Dose Variations

of the greater depth of LH₂ column is also observed by comparison of the dose rate and integral dose curves shown in Figures 9 and 10, with identical curves for the single tank configuration shown in Figures 7 and 8.

The slightly lower tank-top dose levels for the PDL and TCA sources are attributed primarily to the larger source-to-detector separation distance in the hybrid configuration. The relative LH₂ column thickness and aft bulkhead surface geometry characteristics for energy deposition are less effective since the external sources, especially the PDL (and also the TPA if included) are located off the vertical axis of the tank configuration. Consequently, these sources do not derive the maximum benefits from the shadow shielding effect of the LH₂ column. However, since the magnitude of any single external source is considerably less than that of the PVARA source, it is a simpler design task to shield the external sources locally or to relocate the particular component or line if necessary.

Thus, the hybrid configuration employing an upper tank with a reduced cone angle and end cap radius results in relatively low tank-top integral doses primarily due to increased source-to-detector separation distance, since the smaller aft tank adjacent to the NERVA engine is constrained by the size limitations of the space shuttle (used for delivery to orbit) and the propellant requirements for end-of-life engine disposal. The present cargo bay of the space shuttle is sized to have a clear volume of 15-foot diameter by 60-foot length. Therefore, the possible geometrical variations in the design of the small tank are limited if (1) a 9300-9500 pound LH₂ capacity is required and (2) the small tank and NERVA engine are to be launched as a unit with the space shuttle. It is concluded that further reduction of integral tank top dose might be possible by reducing the cone angle and end cap radius of the aft bulkhead of the upper tank in the hybrid configuration, thus elongating the total vehicle configuration. This, in turn would increase the source-to-detector separation distance, and could represent the achievable upper limit for minimization of integral tank top dose with the hybrid configuration under the present RNS ground rules.

However, the subtleties introduced by the coupling of the larger forward tank with a smaller capacity aft tank of larger radius should be examined in greater detail than was possible in this study.

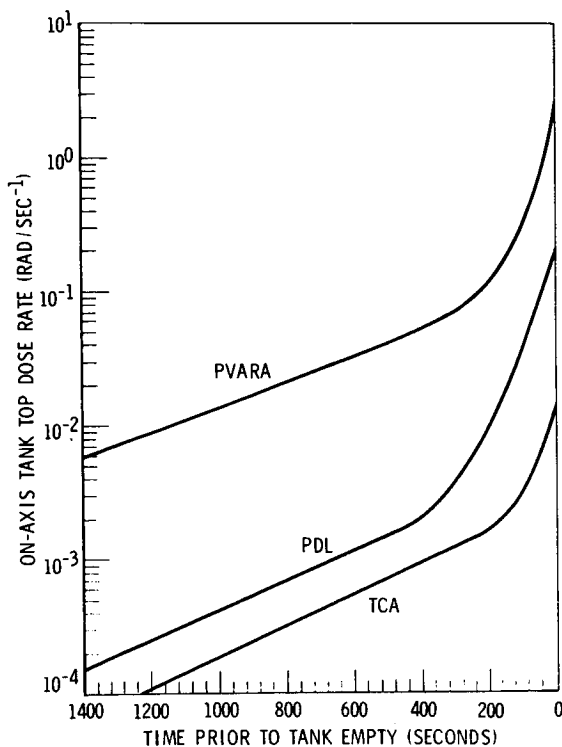


Figure 9. Hybrid-Tank Radiation Dose Rate Variations

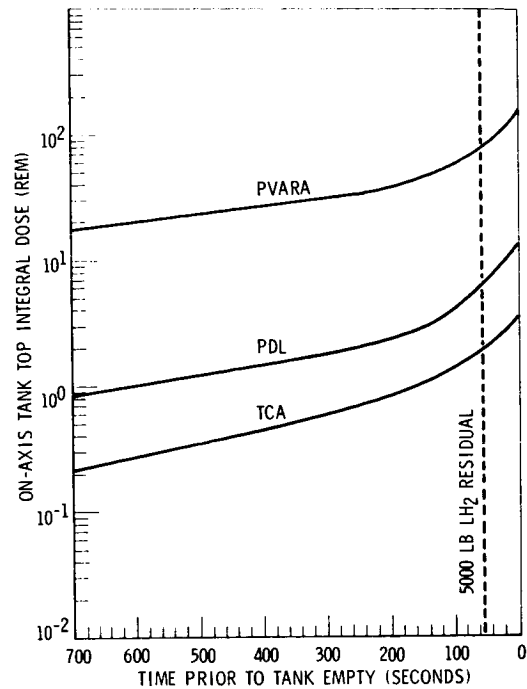


Figure 10. Hybrid-Tank Integral Radiation Dose Variations

SHIELD WEIGHT COMPARISONS TANK CONFIGURATION ANALYSIS

The external shield weights evaluation for the three tentative baseline configurations was based on a nominal 10,000-pound lead disk shield, located 81 inches forward of the core center. The baseline shield design model was taken from March 1970 CRAM data, Reference(4), and is shown in Figure 11. Parametric shield weights as a function of integral tank-top gamma dose were developed utilizing the WANGREV computer program. The external disk shield model was treated by the program in two segments, i.e., a central segment of constant 25-inch radius and varying thickness, and a peripheral section of varying thickness and varying outer radius from 25 to 50 inches. The on-axis integral tank-top dose values shown in Table 4 were utilized as initial dose levels for the computations. Comparative integral dose values as a function of external shield weight for the three tentative baseline configurations are shown in Figure 12. Since the initial integral dose values for the modified dual-cell configuration are almost identical to the single tank configuration, the shielding weights may be considered equivalent for the two configurations for all practical purposes. The curve for external disk weights versus tank top dose for the ANSC 15-degree conical baseline configuration is extrapolated from another study (Reference 8). Since the integral dose levels for this configuration were computed on the basis of a 7500 pound LH₂ residual, the external shield weights were normalized to correspond to a common LH₂ residual of 5000 pounds (Figure 12).

Assuming a payload attenuation factor of 3 (study guidelines and constraints document, Reference 9), an integral tank top dose of 10 rem would be within the allowable dose criteria of 3 rem per crew member, and 10 rem per passenger per round-trip shuttle mission. The external disk-shield weight requirements for an allowable tank top integral dose of 10 rem are summarized in Table 5 for the three tentative baseline configurations as well as the ANSC 15-degree conical configuration and ANSC results for the 10-degree hybrid configuration, both normalized to a common LH₂ residual level of 5000 pounds. Table 5 shows that the baseline single tank conical configuration and modified dual-cell configuration result in the lowest external shield weight requirement of 4050 pounds.

The Space Division hybrid configuration requires an external disk shield weight of 5900 pounds which represents an additional external shield weight penalty of 1850 pounds when compared to the single tank and

modified dual cell baseline configurations. The 10-degree hybrid configuration requires an additional 800 pounds more of external shield weight than the NR-SD hybrid configuration. The ANSC 15-degree conical configuration requires an 11,950 pound external shield based on the aforementioned study criteria. This represents a delta shield weight penalty of about 7800 pounds when compared to Space Division's single conical and modified dual-cell configurations.

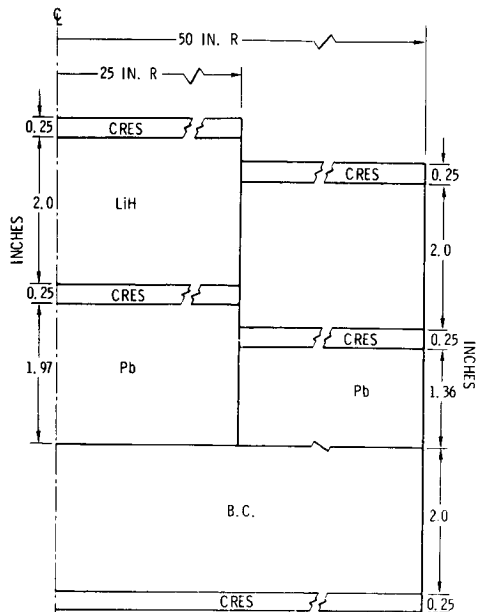


Figure 11. Disk Shield Model with Lead Gamma Shield Region

The after-shutdown gamma kerma rates ($\text{rad}/\text{hour}^{-1}$) following the last engine burn (EOI) are shown in Figure 13. The rates are given at a separation distance of 20 feet from the NERVA core center for three polar angles of 0, 90, and 180 degrees, respectively, for varying after-shutdown decay times.

The gamma kerma rates for after-shutdown decay times of 8 hours, 24 hours, 1 week, and 1 month (Figure 13) are summarized in Table 7. Gamma kerma rates for a nominal engine operating power level of 1575 Mw are also included in Table 7 to illustrate that the dose rates are reduced by about 3.5 to 4 orders of magnitude during the first 8-hour post-shutdown time period. Thereafter, incremental reductions are evidenced for after-shutdown decay times of 24 hours, 1 week, and 1 month, respectively, as illustrated in Figure 13 and Table 7.

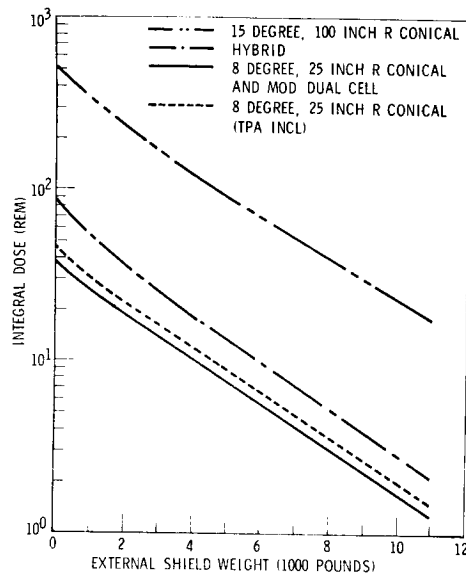


Figure 12. Baseline Shielding Weight Comparison

Table 5. Baseline External Shielding Weight Comparisons

Configuration	External Shield Weight (lbs)	Delta External Shield Weight (lbs)
NR-SD single conical tank 8-degree half cone, 25-inch cap radius (without TPA)	4,050	0
NR-SD modified dual cell	4,050	0
NR-SD 8-degree hybrid	5,900	+1,850
ANSC 15-degree single conical tank	11,950	+7,900
10-degree hybrid (ANSC)	6,700	+2,650
300K lb LH ₂ capacity 5000 lb LH ₂ residual GRAM reference lead disk shield		

RNS MISSION OPERATIONAL CONSIDERATIONS

The preliminary assessment of the after-shutdown radiation from NERVA engine operation was conducted on a representative lunar shuttle mission (Reference 3). Summarily, the shuttle mission entails a total duration of approximately 25 to 27 days with the utilization of four NERVA engine burns during the entire mission cycle. Table 6 itemizes the elements of the mission and their duration. The four engine burns occur in the mission phases identified in the table; (1) translunar injection (TLI), 1750 seconds; (2) lunar orbit insertion (LOI), 310 seconds; (3) transearth injection (TEI), 146 seconds; and earth orbit insertion (EOI), 740 seconds.

Table 6. RNS Representative Lunar Mission

Segment Number	Segment Title	Segment Duration		
		Sec	Min	Sec
1-2	Earth orbital departure (EOD) maneuver			6.44
2-3	Earth orbit departure transfer			43.39
3-4	Earth orbit departure circularization			3.44
4-5	Earth orbit departure orbit			2.08.20
5-6	Translunar injection			29.10
6-7	Translunar injection cooldown			1.00.20.00
7-8	Initial translunar flight			2.00.00
8-9	Translunar injection mid-course correction			14.31
9-10	Final translunar flight			1.18.19.19
10-11	Lunar orbit insertion (LOI)			5.10
11-12	Lunar orbit insertion cooldown			10.16.40
12-13	Lunar orbit rendezvous orbit			8.20.00
13-14	Lunar orbit rendezvous maneuver			33.20
14-15	Lunar orbit operations			17.21.31.38
15-16	Lunar orbit departure (EOD) maneuver			1.11
16-17	Lunar orbit departure transfer			59.25
17-18	Lunar orbit departure circularization			1.11
18-19	Lunar orbit departure orbit			2.46.22
19-20	Transearth injection			2.26
20-21	Transearth injection cooldown			6.40.00
21-22	Initial transearth flight			1.12.06.40
22-23	Transearth injection mid-course correction			8.58
23-24	Final transearth flight			1.0.56.22
24-25	Earth orbit insertion (EOI)			12.20
25-26	Earth orbit insertion cooldown			14.10.00
26-27	Earth orbit rendezvous maneuver			13.53.20
27-28	Earth orbit rendezvous maneuver			1.05

Table 7. After Shutdown Radiation Environment Following EOI Engine Burn

Polar Angle (degrees)	Separation Distance (ft)	Gamma Kerma Rate (rad-hr ⁻¹)				
		Full Power	After Shutdown			
			8 hrs	24 hrs	1 week	1 month
0	20	2.38 x 10 ⁵	2.53 x 10 ¹	8.79	7.45 x 10 ⁻¹	1.51 x 10 ⁻¹
90	20	1.25 x 10 ⁷	7.65 x 10 ³	1.74 x 10 ³	1.92 x 10 ²	3.91 x 10 ¹
180	20	9.37 x 10 ⁶	6.06 x 10 ³	1.42 x 10 ³	1.63 x 10 ²	3.25 x 10 ¹

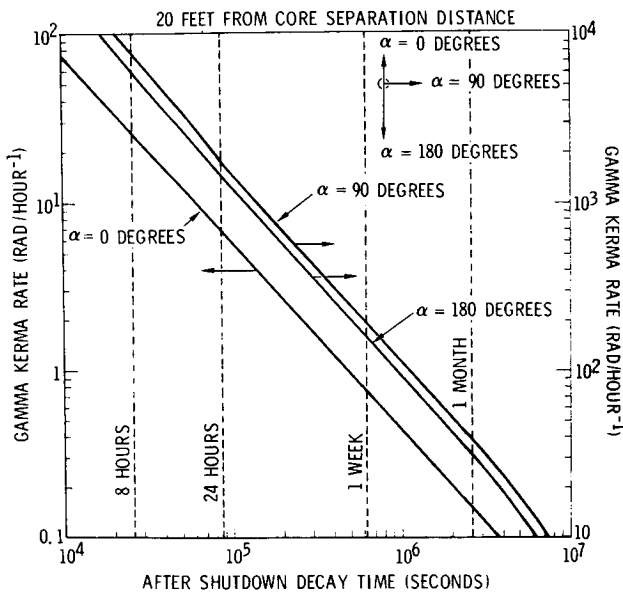


Figure 13. After-Shutdown Radiation Environment

After the fourth engine burn for EOI there is a 14-hour engine cooldown operation prior to the EO rendezvous orbit segment which has a duration of slightly less than 14 hours. After-shutdown isodose contours 24 hours after the EOI engine firing are shown in Figure 14 to further demonstrate a typical after-shutdown radiation environment in the vicinity of the NERVA engine. As in Figure 13, gamma kerma rates (rad/hour⁻¹) are given as a function of separation distance in feet from the engine core midplane with reference to a polar angle, $\alpha = 0$ degrees, along the vertical axis in the forward direction.

Figure 14 illustrates that only minor stage maintenance operations (limited to the 0-15 degree quadrant forward of the engine core midplane) appear to be feasible near the engine-stage interface without additional shielding provisions up to 24 hours after the last engine shutdown cycle. This observation is predicated on the current basic criterion of a 25-rem/year allowable dose to maintenance personnel from the RNS (Reference 9).

For example, an operation involving rendezvous maneuvers with a space tug for engine removal would require rather extensive additional shielding provisions for protection of the crew, remote handling equipment, and manipulative techniques. However, if an unmanned tug vehicle were contemplated for this operation, the primary concern is possible radiation damage to its components, subsystems, and systems due to the aftershutdown gammas from the engine. Integral gamma doses were determined for the removal operation after one and ten RNS lunar mission cycles, respectively, for a 0-degree polar angle orientation between the midplanes of the engine core and tug during the docking maneuver (as well as for a 90-degree orientation). Cumulative gamma doses of 857 rads (C) and 2.43×10^5 rads (C), respectively, were derived for the 0-degree and 90-degree orientations after one complete mission cycle.

For the engine removal after ten mission cycles, integral gamma doses of 2.14×10^3 rads (C) and 6.08×10^5 rads (C) were derived, respectively, for the 0-degree and 90-degree orientations. Thus, the 0-degree orientation of the engine and tug prior to docking affords significant radiation shielding advantages, principally due to the presence of the internal engine shield in the 0-15 degree quadrant with respect to the engine core midplane. Similarly, an additional attenuation factor of 3-4, attainable in the above quadrant if the 4,000-pound external disk shield, is included in the stage configuration. Utilizing the preferred 0-15 degree orientation between the engine and the tug during the docking maneuver, it can be concluded that the integral gamma doses are several orders of magnitude below anticipated

radiation damage thresholds for most of the candidate materials and components. The above calculations assumed a separation distance of 20 feet between the engine core midplane and the location of the nearest tug component. Additionally, it was assumed that the engine removal operation was initiated 24 hours after the last engine burn (EOI) and was terminated one week later with the insertion of the NERVA engine into a 660 n mi "safe" orbit.

It may be concluded that any contemplated manned mission operations (maintenance, repair, logistics, engine removal) involving a near approach to the engine in either the radial or aft directions will dictate additional fixed shielding requirements. These fixed shielding requirements will be significantly reduced (previously shown in Figures 12 and 13 and Table 7) if such operations are performed 8-24 hours after the last engine firing. Tentatively, this doctrine does not appear to compromise presently conceived traffic models or the mission time tables for subsequent shuttle trips.

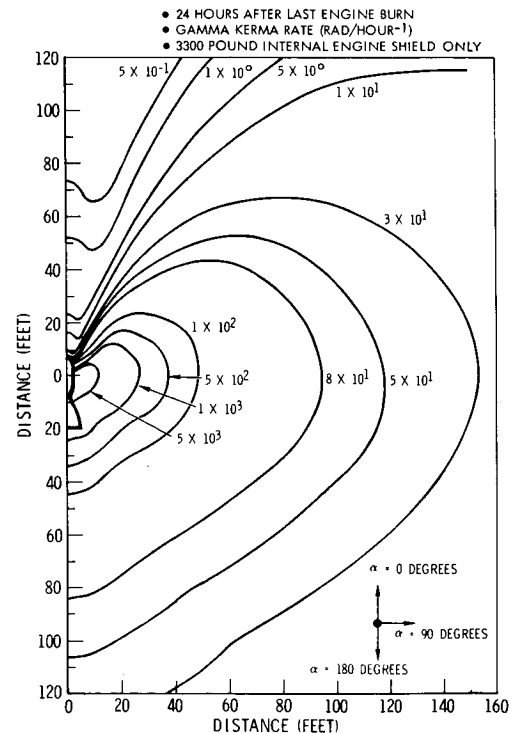


Figure 14. After-Shutdown Iso-Dose Contours

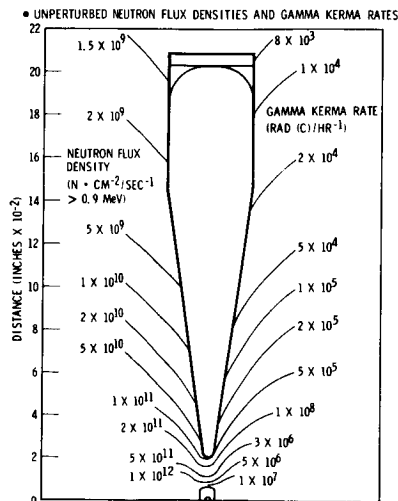


Figure 15. RNS Baseline Configuration - Iso Contours

RADIATION DAMAGE ASSESSMENT

A radiation damage assessment of candidate materials, components, and subsystems has been initiated for the single-tank conical configuration (8-degree half cone-angle and a 25-inch end cap radius). Iso-contour plots of fast neutron flux densities ($E > 0.9$ Mev) and gamma kerma rates are shown in Figure 15 for the single-tank conical configuration as a function of distance from the NERVA engine core midplane. Early analysis indicates that those components located in the forward bulkhead region (astrionics bay) appear to be well protected, in general, by the inherent shield design of the vehicle previously discussed in this paper. In fact, the neutron flux densities are relatively insignificant during the total engine operational cycle due to the appreciable LH₂ column and the large attenuation afforded by the internal and external shields. Similarly, integral tank-top gamma kerma rates would be about 50-75 rad (C) per hour⁻¹ of engine full-power operation or about 500-750 rad (C) for ten RNS lunar missions. Several guidance, navigation and control components (horizon scanners, star trackers, RCS thruster modules, and the rendezvous radar antenna) when deployed appear to be the only components, based on the current design, that would be subjected to higher radiation levels by virtue of their location external to the periphery of the outer tank wall. A neutron fluency of 5.4×10^{13} nvt and integral gamma kerma dose of about 8×10^4 rad (C) appear possible for these components based on unperturbed neutron flux densities and gamma kerma rates from general iso-contour plots for ten RNS lunar mission cycles.

However, those components located in the tank aft bulkhead region will be subjected to appreciably higher radiation levels. In particular, the unattenuated fast neutron flux densities range from about 1×10^{11} to 5×10^{11} n-cm⁻² second⁻¹ and the gamma kerma rates from about 4×10^5 to 9×10^5 rad (C) hour⁻¹ in the region between the tank bottom and the engine and stage interface. For ten RNS lunar missions, this would represent a neutron fluency of about 3.6×10^{14} to 1.8×10^{15} nvt and a gamma kerma dose of about 4×10^6 to 9×10^6 rad (C). Therefore, organic valve seals, gaskets, and organic adhesives in the insulation subsystem, etc., could be marginal in the aforementioned region. Similarly, sensors (liquid level, temperature, pressure transducers), electrical components, and lines must also be more thoroughly evaluated as part of the radiation effects test program. However, none of the aforementioned radiation levels include the additional attenuation afforded by the inclusion of an external disk shield below the engine and stage interface for manned missions.

SUMMARY AND CONCLUSIONS

The single-tank conical and modified dual-cell configurations, both employing aft bulkhead geometries with an 8-degree half cone-angle and a 25-inch end cap radius, represent the configurations with a minimum integral tank-top dose of 37-38 rem and a minimum external shield weight of about 4000 pounds on the basis of an allowable dose criterion of 10 rem at the tank top. However, the insertion of the inner cell in the modified dual-cell configuration creates an additional structural weight penalty of

1275 pounds. From a radiation standpoint, the optimum hybrid configuration exhibits a tank-top integral dose of about 88 rem. The higher integral dose for the hybrid configuration is principally due to larger dose contributions from the PVARA source arising from the geometrical constraints on the small tank adjacent to the NERVA engine. These constraints tend to limit the end cap closure to a radius of 77 to 80 inches to meet the space shuttle's dual requirements of 9300 pounds of LH₂ tank capacity for end-of-life engine disposal, and an allowable cargo volume of 15-foot diameter by 60-foot length for the space shuttle are satisfied. Consequently, further reductions in the tank-top integral dose and, in turn, external shield weight, appear possible for a fixed total propellant capacity by decreasing the aft bulkhead cone-angle and end cap radius of the large forward tank in the hybrid configuration, thereby increasing the source-to-detector separation distance for the total vehicle.

In general, single tank configurations utilizing smaller cone-angles and end cap radii were found to minimize integral radiation levels, and stage shielding-weight penalties for shuttle missions. For a fixed tank propellant capacity this is due to the greater source-to-payload separation distance, reduced effective energy deposition and scattering centers in the aft end of the tank, and greater depth of the liquid hydrogen propellant for radiation attenuation at any given time during the draining cycle.

Hybrid configurations employing an upper tank with smaller cone-angles and end cap radii result in minimum integral payload doses primarily due to increased separation distance, since the smaller aft tank adjacent to the NERVA engine is constrained by the size limitations of the earth-orbital shuttle and the mission propellant requirements.

It may be concluded that any contemplated mission operations involving a near approach to the engine and stage interface area of the RNS in either the radial or aft directions will dictate additional fixed shielding requirements. However, a preferred approach oriented toward the forward end of the vehicle will minimize shielding requirements for such operations as rendezvous, docking, maintenance, and engine disposal.

A preliminary radiation damage assessment of possible RNS materials, components, and subsystems has revealed a number of areas requiring more detailed future examination. The RNS requirement for 10-hour NERVA engine operation imposes detailed perusal of astrionics/electronics, measurement and insulation subsystems as well as materials for gaskets, seals, and adhesives. Replacement of some of the existing candidate stage materials and components with radiation hardened materials and components and/or local shielding appears to present a reasonable design approach.

REFERENCES

1. Malenfant, R.E., "QAD: A series of Point Kernel General Purpose Shielding Programs," Los Alamos Scientific Laboratory, LA-3573 (October 1966).
2. Seminar/Workshop Material on Kernel Techniques for Nuclear Rocket Propellant Tank Geometry/Shielding Analysis (U), Aerojet-General Corporation, RN-PA-0020 (8 and 19 August 1969).
3. Nuclear Flight System Definition Study, Phase II Final Report, Volume III - Systems Definition - Requirements and Systems Analysis, Space Division, North American Rockwell Corporation, SD 70-117-3 (August 1970).
4. Full Flow-Flight Engine Common Radiation Analysis Model (U), Aerojet General Corporation, RN-S-0551 (6 March 1970). (Confidential)
5. Nuclear Shuttle Definition Study - Phase III First Interim Review, Space Division, North American Rockwell Corporation, PDS-70-242 (September 2, 1970).
6. Warman, E.A. and K.O. Koebberling, Monte Carlo Analysis of North American Rockwell Propellant Tank, S100-TM04-W118 (November 1970).
7. Nuclear Shuttle Definition Study - Phase III Second Interim Review, Space Division, North American Rockwell Corporation, SD 70-644 (16 December 1970).
8. Radiation Analysis of Various Vehicles and Payloads for the Reusable Nuclear Shuttle, Aerojet Nuclear Systems Company S100-TRA06-W118-12 (August 1970).
9. Guidelines and Constraints Document - Nuclear Shuttle Systems Definition Study, Phase A, MSFC Document No. PD-SA-P-70-63, Rev. No. 2 (October 1 1970).